

## RESEARCH ARTICLE

# Development of novel quality control material based on CRISPR/Cas9 editing and xenografts for MLH1 protein deficiency testing

Rui Li<sup>1,2,3</sup> | Runling Zhang<sup>1,2,3</sup> | Ping Tan<sup>1,2,3</sup> | Meng Wang<sup>1,2,3</sup> | Yuqing Chen<sup>1,2,3</sup> |  
Jiawei Zhang<sup>1,2,3</sup> | Dongsheng Han<sup>1,2,3</sup> | Yanxi Han<sup>1,3</sup> | Jinming Li<sup>1,2,3</sup>  |  
Rui Zhang<sup>1,2,3</sup> 

<sup>1</sup>National Center for Clinical Laboratories, Beijing Hospital, National Center of Gerontology; Institute of Geriatric Medicine, Chinese Academy of Medical Sciences, Beijing, China

<sup>2</sup>Graduate School of Peking Union Medical College, Chinese Academy of Medical Sciences, Beijing, China

<sup>3</sup>Beijing Engineering Research Center of Laboratory Medicine, Beijing Hospital, Beijing, China

## Correspondence

Rui Zhang, and Jinming Li, National Center for Clinical Laboratories, Beijing Hospital, No.1 Dahua Road, Dongdan, 100730 Beijing, China.  
Emails: ruizhang@nccl.org.cn (RZ); jmli@nccl.org.cn (JL)

## Funding information

National Key R&D Program of China, Grant/Award Number: 2018YFE0201604; the Fund for Beijing Dongcheng District Outstanding Talents Team Program, Grant/Award Number: 2019DCT-M-01; Beijing Hospital Nova Project, Grant/Award Number: BJ-2018-136

## Abstract

**Background:** Mismatch repair deficiency (dMMR) status induced by MLH1 protein deficiency plays a pivotal role in therapeutic decision-making for cancer patients. Appropriate quality control (QC) materials are necessary for monitoring the accuracy of MLH1 protein deficiency assays used in clinical laboratories.

**Methods:** CRISPR/Cas9 technology was used to edit the *MLH1* gene of GM12878Cas9 cells to establish MLH1 protein-deficient cell lines. The positive cell lines were screened and validated by Sanger sequencing, Western blot (WB), and next-generation sequencing (NGS) and were then used to prepare formalin-fixed, paraffin-embedded (FFPE) samples through xenografting. These FFPE samples were tested by hematoxylin and eosin (H&E) staining and immunohistochemistry (IHC) for suitability as novel QC materials for MLH1 protein deficiency testing.

**Results:** We successfully cultured 358 monoclonal cells, with a survival rate of 37.3% (358/960) of the sorted monoclonal cells. Through Sanger sequencing, cell lines with *MLH1* gene mutation were identified. Subsequently, two cell lines with MLH1 protein deficiency were identified by WB and named as GM12878Cas9\_6 and GM12878Cas9\_10. The NGS results further confirmed that the *MLH1* gene mutation in these two cell lines would cause the formation of stop codons and terminate the expression of the MLH1 protein. The H&E staining and IHC results also verified the deficiency of the MLH1 protein, and FFPE samples from xenografts proved their similarity and consistency with clinical samples.

**Conclusions:** We successfully established MLH1 protein-deficient cell lines. Followed by xenografting, we developed novel FFPE QC materials with homogenous, sustainable, and typical histological structures advantages that are suitable for the standardization of clinical IHC methods.

Rui Li and Runling Zhang contributed equally to the work.

This is an open access article under the terms of the Creative Commons Attribution-NonCommercial-NoDerivs License, which permits use and distribution in any medium, provided the original work is properly cited, the use is non-commercial and no modifications or adaptations are made.

© 2021 The Authors. *Journal of Clinical Laboratory Analysis* published by Wiley Periodicals LLC

## KEYWORDS

CRISPR/Cas9, immunohistochemistry, MLH1, next-generation sequencing, quality control material

## 1 | INTRODUCTION

With the development of immune checkpoint inhibitor (ICI) therapies, mismatch repair deficiency (dMMR) has become a predictive biomarker to distinguish cancer patients who may benefit from these therapies, and it is the first tissue/site-agnostic biomarker approved by the Food and Drug Administration (FDA).<sup>1–4</sup> The mismatch repair (MMR) system is an important DNA repair mechanism that allows the cell to quickly identify and repair base-base mismatches and insertion/deletion errors generated during DNA replication and recombination.<sup>5,6</sup> The main genes involved in the MMR system are *MLH1*, *PMS2*, *MSH2*, and *MSH6*.<sup>7</sup> Mutations in any of these genes or methylation in the *MLH1* gene promoter will trigger dMMR, which will lead to deficiency of the MMR protein and inability to repair errors that occur during DNA replication. Studies have shown that dMMR induced by *MLH1* protein deficiency could be found in 8–21% of colorectal cancers<sup>8,9</sup> and 24–37% of endometrial cancers.<sup>10,11</sup> A study that included 1,048 colorectal cancer patients showed that *MLH1*, *MSH2*, or *MSH6* protein deficiency was found in 9.8%, 1.4%, and 0.5% of patients, respectively, indicating that protein deficiency caused by *MLH1* gene mutation had a higher incidence in colorectal cancer than other MMR genes (*MSH2*, *MSH6*).<sup>12</sup> Therefore, accurate detection of *MLH1* protein deficiency in cancer patients is critical to clinical decision-making.

In the clinic, immunohistochemistry (IHC) of tumor tissue samples is the standard first-line screening tool recommended for dMMR detection.<sup>13</sup> As one of the most commonly used molecular diagnostic techniques, IHC has the advantages of ease of performance and high cost-effectiveness, and it can also identify the mutated gene.<sup>14</sup> At present, the sensitivity and specificity of IHC for detecting *MLH1* protein expression are 80% and 90%–95%, respectively.<sup>15–17</sup> However, IHC is a multi-step process, and many aspects of the detection process (ie, antigen retrieval, selection and preparation of antibody and reagents, incubation, washing, and counterstaining) can affect its performance and result in substantial variability. In a study on evaluation of IHC performance, Muller et al. reported that *MLH1* staining was inconsistent in multiple laboratories, mainly due to technical factors.<sup>18</sup> Antigen retrieval and antibody incubation are considered the two key points associated with successful staining. Excessive microwave exposure can destroy the antigenicity and cell morphology of the tissue, affect the staining results, and cause weak or absent staining.<sup>19</sup> Different manufacturers of antibody clones and improper antibody dilution and incubation time influence the final staining effect.<sup>20</sup> Other factors, such as excessive hydrogen peroxide incubation time and inconsistent setting of the cutoff value of the tumor cell nuclear staining percentage, have varying degrees of influence on the interpretation of the results.<sup>21</sup> Therefore, there are many pitfalls of the IHC assay due to differences in staining platforms, antibody clones, scoring systems, and quality control (QC) materials that are required to analyze and verify the testing process to standardize the clinical testing.

At present, there are two kinds of commonly used QC materials for IHC testing: formalin-fixed, paraffin-embedded (FFPE) tumor tissues from clinical tumor patients<sup>22,23</sup> and immortalized tumor cell lines.<sup>24,25</sup> There is no doubt that FFPE tumor tissues from tumor patients can accurately represent authentic human cancer. However, the main challenges of using such materials are that the source of solid tumor tissue is limited and that the tumor tissues are heterogeneous among different individuals. This makes it difficult to obtain a large number of tumor tissue samples with good reproducibility as QC materials. Immortalized tumor cell lines are also not a perfect alternative. Although a large number of immortalized cell lines can be obtained, their source is limited to specific tumor types, mainly cultured from existing patient tumor tissues.<sup>24</sup> FFPE cell line samples usually lack histological structure, making it difficult to represent the complexity of the tissue, and it is possible for the cells to slip off the slide during processing.<sup>24</sup> In addition, highly consistent and low-cost synthetic biomaterials, such as synthetic peptides, have also been developed.<sup>26</sup> By incorporating synthetic peptides into a homogeneous protein gel of known composition, a gel containing antigen was developed as a QC material, similar to a paraffin-embedded tissue block.<sup>27</sup> However, these biomaterials can only be used to evaluate only the performance of one or a few steps (such as staining and antigen retrieval) in IHC testing and lack cell and tissue structures. Therefore, considering the limitations of current QC materials, it is necessary to establish a novel FFPE QC material with good characteristics that is available in large quantities.

CRISPR-mediated targeted gene editing technology can overcome the limitations of existing QC materials with respect to tumor tissue types and sources, especially when used in immortalized cell line samples<sup>28–30</sup> and it has become a valuable method for the preparation of QC materials with good reproducibility and in large quantities. FFPE materials prepared from edited cell lines by xenografting can produce typical histological structures similar to those found in tumor tissues, such as in *EML4-ALK* rearrangement.<sup>31</sup> In this study, we have combined CRISPR/Cas9 and xenotransplantation technology to establish *MLH1* protein-deficient cell lines and to develop novel FFPE QC materials for evaluating the capabilities of laboratory IHC detection of the *MLH1* protein. Moreover, our work provides new insight into preparing QC materials for the MMR system, and this approach may also be suitable for other MMR proteins, such as *PMS2*, *MSH2*, and *MSH6*.

## 2 | MATERIALS AND METHODS

### 2.1 | sgRNA design and in vitro transcription

Based on sgRNA databases for *MLH1* gene knockout (Human\_GeCKOv2\_Library) and a previous study,<sup>32</sup> we used CRISPOR software to analyze and select 4 sgRNAs with high scores to knock out the *MLH1* gene to achieve *MLH1* protein deficiency (Table 1).

TABLE 1 Primers used in generation of *MLH1* knockout cell lines

Name	Forward primer	Reverse primer
Primers for in vitro transcription of <i>MLH1</i> sgRNA		
MLH1-F1	5'-TAATACGACTCACTATAGG <b>GCGAATATTGTCCACGGTTG</b> GTTTTAGAGCTAGAAATAGC-3'	5'-GCACCGACTCGGTGCCACTT-3'
MLH1-F2	5'-TAATACGACTCACTATAGG <b>TACCATTCTTACCGTGATCT</b> GTTTTAGAGCTAGAAATAGC-3'	
MLH1-F3	5'-TAATACGACTCACTATAGG <b>AGACAATGGCACCGGGATCA</b> GTTTTAGAGCTAGAAATAGC-3'	
MLH1-F4	5'-TAATACGACTCACTATAGG <b>CACATCGAGAGCAAGCTCCT</b> GTTTTAGAGCTAGAAATAGC-3'	
Primers to amplify target sites for T7E1 assay		
MLH1sgRNA-1P	5'-TCTGAAGCATAAAACAAGCCT-3'	5'-ATCAGCAACCTATAAAAGTAGAGA-3'
MLH1sgRNA-2P	5'-GACCTCCATTAAGTAGTGCAA-3'	5'-GAACTCAGCAAGTAAATAGCAAC-3'
MLH1sgRNA-3P	5'-GCCTGTAAGACAAAGGAAAAACACGTTA-3'	5'-ATTACTCTTTCCTTTTCAGCCTTAGACAA-3'
MLH1sgRNA-4P	5'-CCTGACAGTTTAGAAATCAGTCCCC-3'	5'-CTAGTCACACGGCTGGTAACCC-3'

Note: The sgRNA sequences in Table 1 are marked in red.

Using a plasmid containing the scaffold-associated region of the full sgRNA skeleton-related region as a template, the T7 RNA polymerase promoter and specific target sequences were added to the sgRNA sequences by polymerase chain reaction (PCR). The specific forward primers and universal reverse primers used in the PCR are listed in Table 1. The MEGAshortscript™ T7 Transcription Kit synthesis kit (Thermo Fisher Scientific Inc., Waltham, MA) was used for in vitro transcription. The obtained sgRNAs were purified with the MEGAclean kit (Thermo Fisher Scientific Inc.), eluted in nuclease-free water, and stored at  $-80^{\circ}\text{C}$  until use.

## 2.2 | Cell culture and electroporation

GM12878 cells stably expressing Cas9 and mCherry were donated by the Wensheng Wei Laboratory. The cells were cultured in RPMI-1640 medium containing 10% fetal bovine serum, 100  $\mu\text{g}/\text{ml}$  streptomycin, and 100 IU penicillin (all from Thermo Fisher Scientific Inc.) at  $37^{\circ}\text{C}$  and 5%  $\text{CO}_2$ . Cas9-expressing GM12878 cells were resuspended in the electroporation buffer (Celetrix LLC, Manassas, VA) at a density of  $1\text{--}1.5 \times 10^6/\text{ml}$ , and 12  $\mu\text{g}$  of in vitro transcribed *MLH1*sgRNA1-4 was added to the cells. After mixing, 20  $\mu\text{l}$  was transferred to 20- $\mu\text{l}$  electroporation tubes. Electroporation was then performed at 400 V for 30 ms. After electroporation, the cells were immediately transferred into  $37^{\circ}\text{C}$  warmed medium for further culture.

## 2.3 | Validation of mixed clonal cells

The cleavage efficiencies of different sgRNAs were identified using a T7E1 assay at 3–4 days after electroporation. The genomic DNA of the mixed clonal cells was extracted using the Quick Extract DNA extraction solution (Epicenter, Wisconsin, USA), and the DNA

concentration was measured with an Eppendorf BioPhotometer. The T7E1 assay using T7 Endonuclease I (NEW ENGLAND BioLabs Inc., Ipswich, UK) was performed according to the manufacturer's instructions. The PCR system includes 25  $\mu\text{l}$  of PrimeStar Max DNA polymerase (Takara Bio Inc., Shiga, Japan), 1.5  $\mu\text{l}$  of T7E1 forward and reverse primers, 200 ng of cell genomic DNA, and nuclease-free water to make up a 50  $\mu\text{l}$  reaction system. The amplification conditions were as follows:  $98^{\circ}\text{C}$  for 3 min; 35 cycles at  $98^{\circ}\text{C}$  for 10 s,  $53^{\circ}\text{C}$  for 5 s,  $72^{\circ}\text{C}$  for 35 s; and reaction at  $72^{\circ}\text{C}$  for 2 min. After amplification, electrophoresis was performed on a 2% agarose gel to evaluate the cleavage efficiencies.

## 2.4 | Monoclonal cell screening

The mixed clonal cells transfected with the sgRNA having the highest cutting efficiency and with a high mCherry fluorescence signal were sorted into 96-well plates (Corning, Corning, NY) using MoFlo®XDP-SX (XDP, Beckman Coulter). After culturing for 2–3 weeks at  $37^{\circ}\text{C}$  and 5%  $\text{CO}_2$ , the monoclonal cells with CRISPR/Cas9-mediated deletion were rapidly screened by PCR using the amplification conditions described in above section. PCR products purified from positive clones were subsequently verified by Sanger sequencing.

## 2.5 | Detection of cell lines with *MLH1* protein deficiency by Western blot and next-generation sequencing

*MLH1* protein expression in screened monoclonal cells was assessed using Western blot (WB) and next-generation sequencing (NGS). For WB, the monoclonal cells were lysed with 500  $\mu\text{l}$  of RIPA lysis buffer (Solarbio, Beijing, People's Republic of China). Lysates were separated

by SDS-PAGE with an 8% separation gel and 5% concentration gel. After transferring to polyvinylidene difluoride (PVDF) membranes, blots were probed with the primary antibodies (rabbit anti-MLH1 (BD Bioscience, Franklin Lakes, New Jersey; 1:100000) and mouse anti- $\beta$ -actin (CWBio, Beijing, People's Republic of China; 1:5000) polyclonal antibodies), followed by secondary antibodies (mouse anti-rabbit IgG (Santa Cruz Bio Inc., Dallas, Texas; 1:5000) and goat anti-mouse IgG (Santa Cruz Bio Inc.; 1:5000)). GM12878Cas9 and HCT116 cell lines were used as positive and negative controls, respectively. For NGS, genomic DNA was extracted from monoclonal cells using the QIAamp DNA Mini Kit (Qiagen, Hilden, Germany), and 80–120 ng of DNA was used as input for the library preparation. A pool of oligos specific to 523 genes (TruSight Oncology 500 Kit, Illumina, Santiago, Chile) was used to prepare DNA libraries for sequencing on the Illumina NextSeq 550 platform. All procedures were performed following the manufacturer's instructions. Data analysis was performed using the TSO500 module in the commercial software (Illumina).

## 2.6 | Establishment of xenograft models

Female NOD-SCID mice between 4 and 5 weeks of age were selected to establish a xenograft model (Beijing Vital River Laboratory Animal Technology Co., Ltd., Beijing, People's Republic of China). Cell suspension ( $5 \times 10^7$ /ml) was used to subcutaneously inoculate mouse double axilla, with 0.1 ml of cell suspension used on each side. The xenograft tumor volume was measured twice a week with a Vernier caliper. When the xenograft tumor volume reached approximately 1,000 mm<sup>3</sup>, the mice were euthanized, and the xenografted tumors were surgically removed and harvested immediately to prepare the FFPE blocks. The procedures of animal study comply with the guidelines of the Care and Use of Laboratory Animals issued by the Ministry of Science and Technology of China.

## 2.7 | Histological and immunohistochemistry analysis of FFPE samples with MLH1 protein deficiency

Each FFPE block was cut into 3- $\mu$ m-thick slices for hematoxylin and eosin (H&E) and IHC staining. The histomorphology and cytomorphology of each FFPE tumor tissue were visualized by H&E staining. The tumor areas and histological structures were evaluated by a pathologist. IHC was performed on FFPE samples taken from cell lines and xenograft samples. MLH1 and PMS2 protein expression levels were assessed using a commercial kit (ZSGB-BIO, Beijing, People's Republic of China). After paraffin sections were dewaxed and hydrated with xylene and ethanol at different concentrations, dewaxed sections were heated for approximately 20 min in pH 9.0 EDTA antigen retrieval solution (ZSGB-BIO) in a microwave oven. After cooling, the primary and secondary antibodies in the commercial

kit were applied and incubated for 70 min and 20 min, respectively, according to the manufacturer's instructions. A DAB kit (ZSGB-BIO) was used for the final color reaction, and hematoxylin was used for counterstaining. Tumors showing loss of nuclear staining were classified as negative for protein expression. GM12878Cas9 and HCT116 cell lines were used as external positive and negative controls, respectively.

## 3 | RESULTS

### 3.1 | Generation of MLH1 gene mutant cells using the CRISPR/Cas9 system

The CRISPR/Cas9 system was used to edit Cas9-expressing GM12878 cells to generate *MLH1* gene mutant cells through non-homologous end joining (NHEJ). We transfected 4 different sgRNAs targeting the exon regions by electroporation (*MLH1*sgRNA-1, *MLH1*sgRNA-2, *MLH1*sgRNA-3, *MLH1*sgRNA-4) to select the most efficient one (Table 1). Through the T7EI assay, *MLH1*sgRNA-3 and *MLH1*sgRNA-4 interacting with Cas9 were determined to successfully cut the *MLH1* gene, and specific cutting bands appeared, as shown by the red arrow in Figure 1. As the cleavage efficiency of *MLH1*sgRNA-4 was higher than that of *MLH1*sgRNA-3 (Figure 1), the mixed clonal cells transfected with *MLH1*sgRNA-4 and with a high mCherry fluorescence signal were subjected to monoclonal sorting by flow cytometry.

### 3.2 | Validation of monoclonal cells with MLH1 gene mutations and protein deficiency

Through flow cytometry, we obtained 960 monoclonal cells for culture, and we successfully cultivated 358 of these monoclonal cells, for a cell survival rate of 37.3% (358/960). To select positive monoclonal cells, Sanger sequencing, WB, and NGS were performed (Figures 2 and 3). The sequencing results were aligned to the reference sequence of the *MLH1* gene of the human genome sequence (GRCh38/hg38), and cell lines with induced mutations in the *MLH1* gene were identified. In addition to homozygous mutations, we also observed that two overlapping traces were obtained starting at the mutation site by direct Sanger sequencing, demonstrating that heterozygous or bi-allelic mutations were generated (Figure 2A). Through WB detection of the cell lines with sequencing mutations, two cell lines with complete *MLH1* protein deficiency were identified and named as GM12878Cas9\_6 and GM12878Cas9\_10 (Figure 2B). Subsequently, NGS was performed on GM12878Cas9\_6 and GM12878Cas9\_10 *MLH1* protein-deficient cell lines to further clarify the *MLH1* gene mutation and protein deficiency. As expected, both *MLH1* protein-deficient cell lines showed bi-allelic mutations in the region targeted by sgRNA (Figure 3A). Different insertion and deletion mutations leading to

**FIGURE 1** T7EI assay results of mixed clones for detecting the cleavage efficiency of MLH1 sgRNA. Specific DNA bands caused by CRISPR/Cas9 cleavage are marked using red arrows

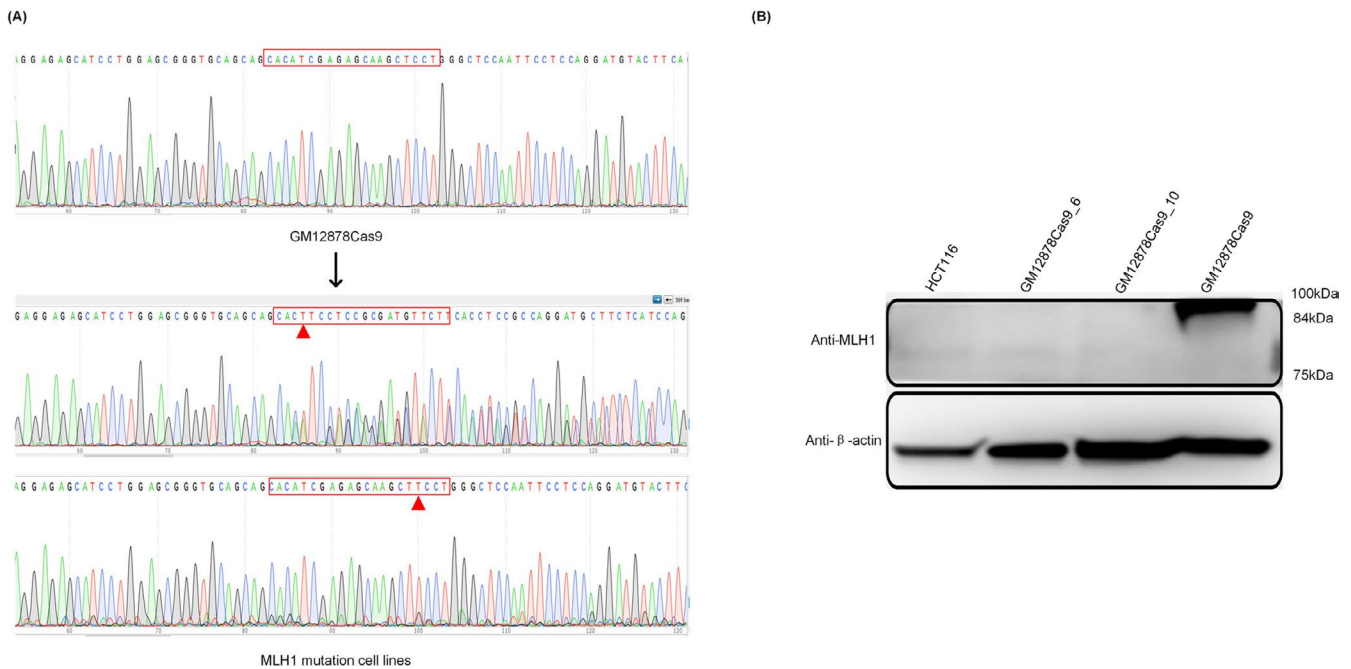
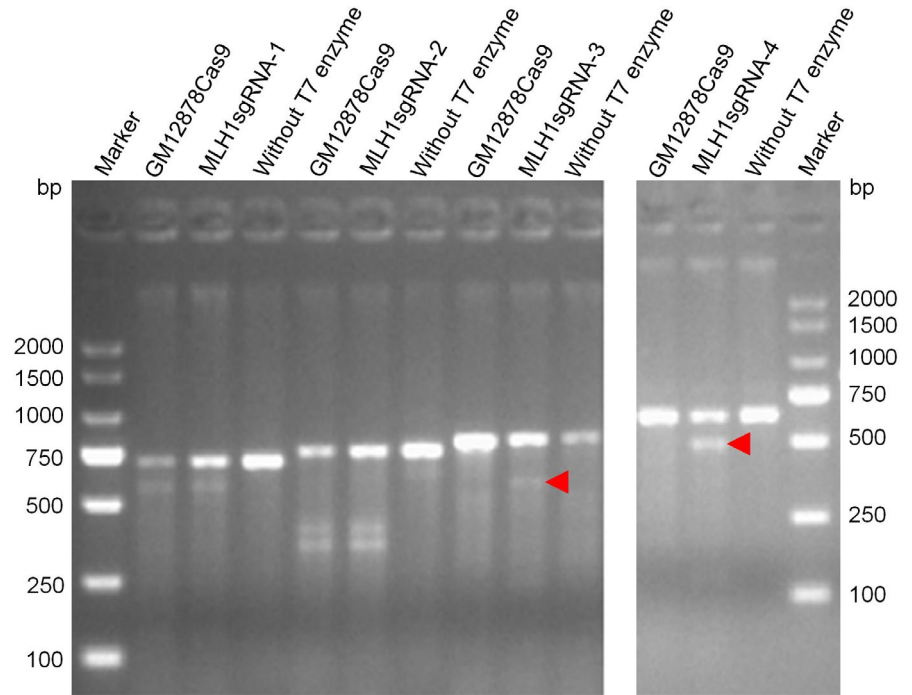


**FIGURE 2** Sanger sequencing and Western blot (WB) results of monoclonal cell lines based on CRISPR/Cas9 technology. (A) The Sanger sequencing results of monoclonal cells. The MLH1sgRNA target site is marked in a red box. Cell lines with mutations in the MLH1 gene showing insertion mutations and two overlapping traces starting at the mutation site were obtained, as shown in A. (B) The WB results of monoclonal cells. The MLH1 protein expression profiles of GM12878Cas9\_6 and GM12878Cas9\_10 cell lines were negative

different forms of termination of MLH1 protein expression were observed (Figure 3B). In the GM12878Cas9\_6 cell line, two allelic mutation forms (c.987\_1012delCATCGAGAGCAAGCTCCTGGGC TCCA; c.1002\_1006delCCTGG) of MLH1 were observed, with mutation frequencies of 52.3% and 40.1%, respectively. One of the protein changes was the conversion of histidine at position 329 to

glutamic acid, resulting in the formation of a stop codon 24 amino acids later (His329GlnfsTer24). The other was the conversion of glycine at position 336 to glutamic acid, resulting in the formation of a stop codon 24 amino acids later (Gly336GlnfsTer24). In the GM12878Cas9\_10 cell line, the two alleles of MLH1 showed a homozygous mutation (c.1001dupT) with a mutation frequency of

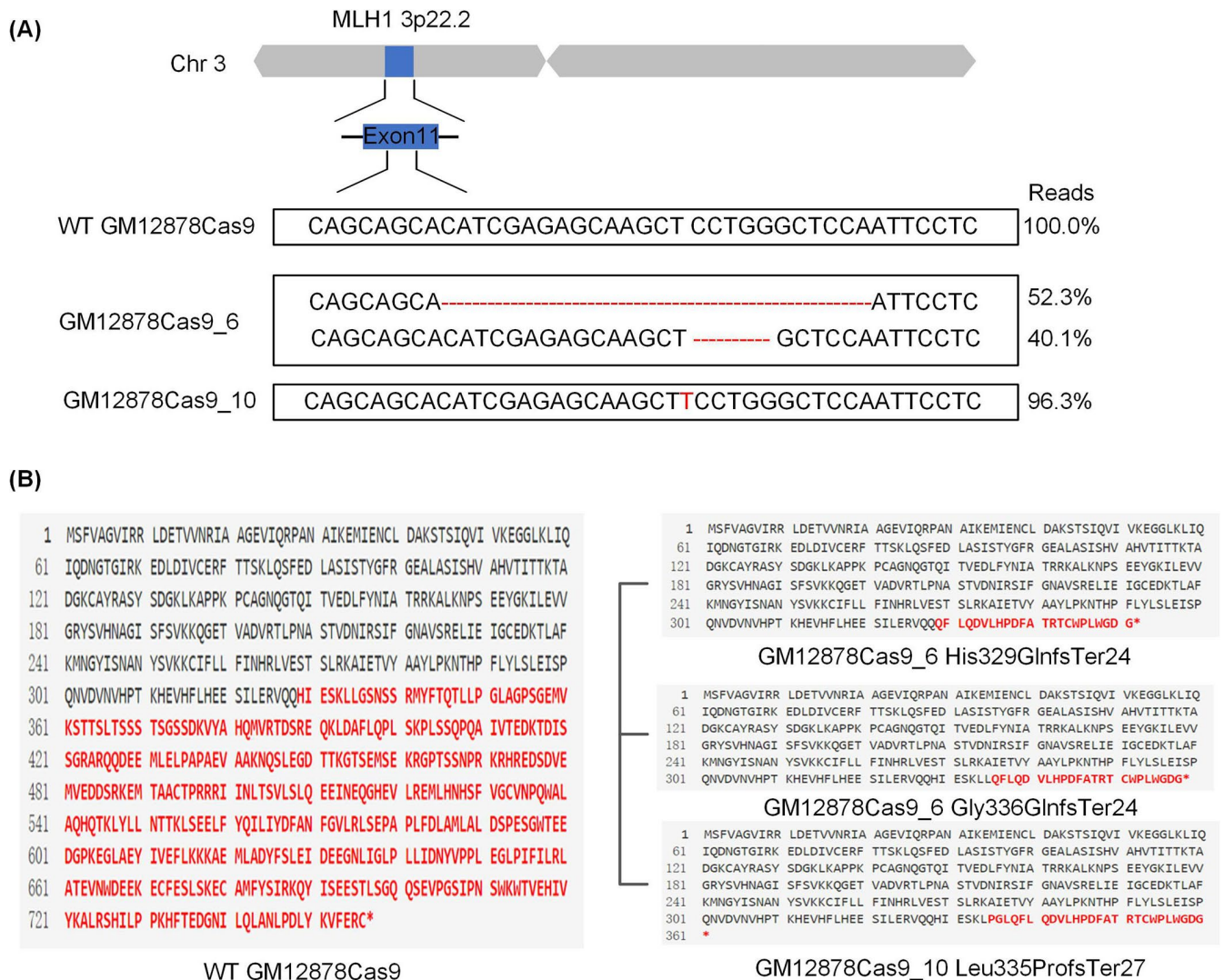


**FIGURE 3** Next-generation sequencing (NGS) results of MLH1 protein-deficient cell lines. (A) The results of *MLH1* gene mutation in MLH1 protein-deficient cell lines (GM12878Cas9\_6 and GM12878Cas9\_10). (B) The results of *MLH1* protein changes in MLH1 protein-deficient cell lines (GM12878Cas9\_6 and GM12878Cas9\_10). Analysis showed that mutations in the *MLH1* gene led to the formation of stop codons, causing truncation mutations in the MLH1 protein

96.3%; the protein expression consequence was the conversion of tyrosine at position 335 to proline, resulting in the formation of a stop codon 27 amino acids later in both alleles (Leu335ProfsTer27).

### 3.3 | Validation of MLH1 protein-deficient cell lines and xenograft samples

The two MLH1 protein-deficient cell lines were further validated by the IHC method. After sectioning, MLH1 protein expression was detected using a ZSGB-BIO commercial kit. The HCT116 and GM12878 Cas9 cell lines were used as negative and positive controls, and the nuclear staining was consistent with expectations, as shown in Figure 4. In detail, there was a distinct loss of nuclear staining in GM12878Cas9\_6 and GM12878Cas9\_10 cells, consistent with the HCT116 cell line, while unedited GM12878 Cas9

showed strong nuclear staining (Figure 4A). These findings indicated that the established MLH1 protein-deficient cell lines were suitable for IHC detection. Subsequently, mouse xenograft samples with MLH1 protein-deficient cell lines were also obtained, and the results are shown in Figure 4B,C. We transplanted MLH1 protein-deficient cells into female NOD-SCID mice and induced tumor formation. The tumor volume grew to approximately 1,000 mm<sup>3</sup> within a 3-week time course (Figure 4B). The FFPE samples prepared from xenograft tumor tissues were identified using H&E and IHC staining to determine whether the FFPE samples were similar to clinical samples. The H&E staining results showed that FFPE samples of xenograft tumors had typical histological structures similar to clinical specimens from endometrial cancer patients (Figure 4C a–e) in terms of tumor infiltration, inflammation, bleeding, and tissue necrosis, and the percentage of tumor infiltration on the FFPE slide ranged from 40% to 70%. When detected by

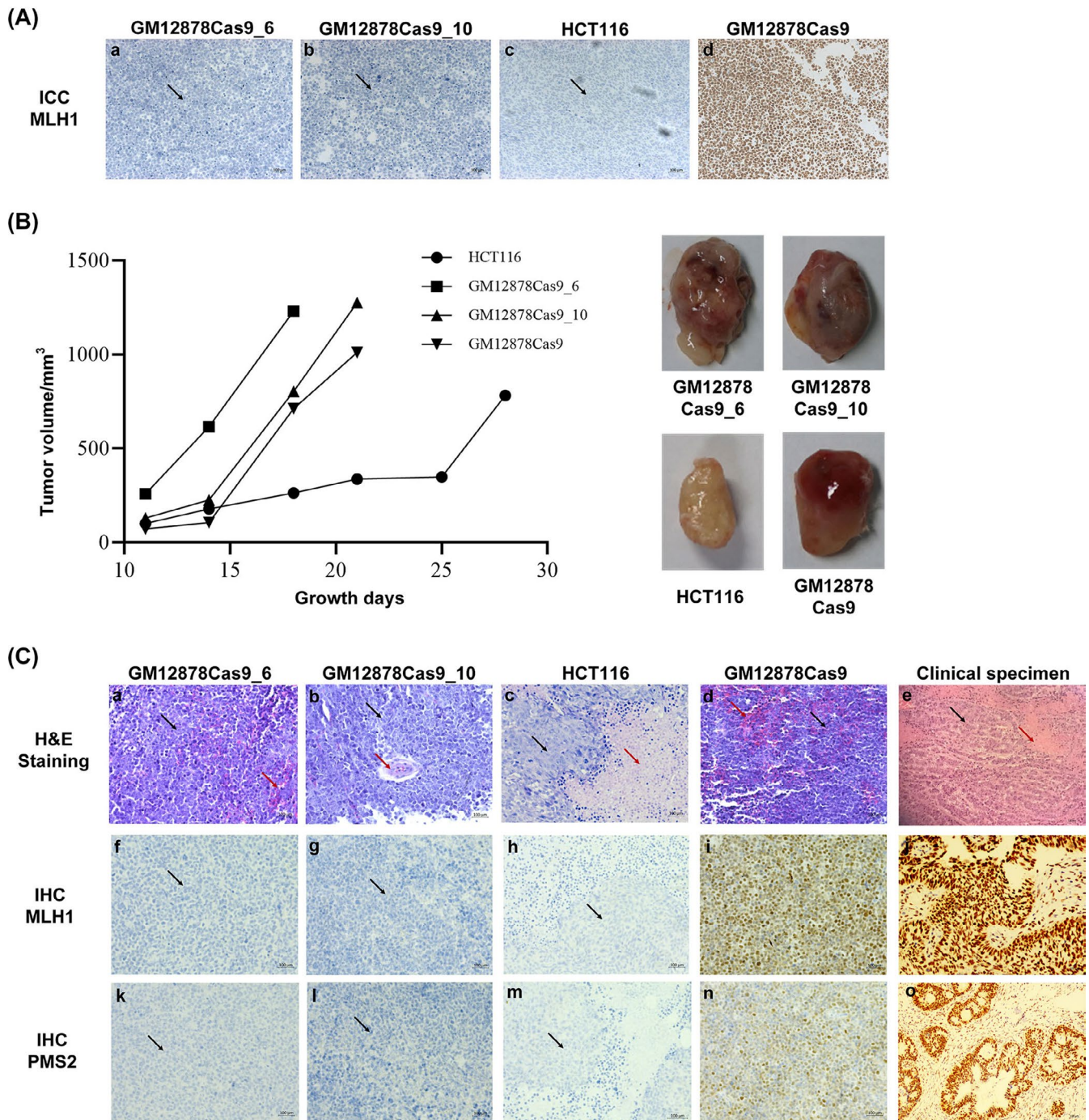


**FIGURE 4** Hematoxylin and eosin (H&E) and immunohistochemical (IHC) staining of MLH1 and PMS2 in MLH1 protein-deficient cell lines and xenograft tumors. (A) Nuclear staining showed that there was a distinct loss of nuclear staining in GM12878Cas9\_6 and GM12878Cas9\_10 cells, consistent with that in the HCT116 cell line, while unedited GM12878 Cas9 showed strong nuclear staining. (B) The tumor volume grew to approximately 1,000 mm<sup>3</sup> within a 3-week time course. (C) H&E and IHC staining showed that FFPE samples of xenograft tumors had typical histological structures similar to those of clinical specimens from endometrial cancer patients. The nuclear staining profiles of MLH1 and PMS2 proteins were all distinctly lost in xenograft tissues samples. The red arrow indicates bleeding, vascular infiltration, and necrosis in H&E-stained tissue; the black arrow indicates MLH1 protein-deficient cells with negative staining by the IHC method

IHC, MLH1 nuclear staining profiles in HCT116, GM12878Cas9\_6 and GM12878Cas9\_10 xenograft tissue samples were all distinctly lost, and no significant difference was observed between the three tissues (Figure 4 f-h). Moreover, we also observed that the nuclear

staining of PMS2, the obligatory partner of the functional complex of MutL $\alpha$ , in HCT116, GM12878Cas9\_6 and GM12878Cas9\_10 xenograft tissue samples was lost, demonstrating the above cell lines were MLH1-/PMS2-deficient phenotype (Figure 4C k-m).

## 4 | DISCUSSION

dMMR induced by MLH1 protein deficiency is an important biomarker that plays a pivotal role in therapeutic decisionmaking for cancer patients, especially for colorectal and endometrial cancers.<sup>3,4,33</sup> Ensuring the accuracy and reproducibility of MLH1 protein deficiency tests requires reliable QC materials for monitoring assay sensitivity and specificity. In this study, we provided a platform to construct MLH1 protein-deficient cell lines based on the CRISPR/Cas9 editing method that may also be used to construct other similar dMMR cell lines with MSH2, MSH6, or PMS2 gene mutations. Importantly, we have also established xenograft models of these cell lines to generate FFPE samples, which can be used as novel QC materials for clinical testing standardization.

Transfection with sgRNA fragment into cells stably expressing Cas9 has proven to be an efficient and convenient CRISPR/Cas9 editing method, which can reduce the cost of plasmid synthesis and shorten the time of plasmid preparation, and has been successfully applied to the preparation of  $\alpha$ -thalassemia QC material.<sup>30</sup> In this study, by editing Cas9-expressing GM12878 cells using sgRNA fragment, we successfully established two MLH1 protein-deficient cell lines, GM12878Cas9\_6 and GM12878Cas9\_10. Notably, in our study, the survival rate of monoclonal cultures was only 37.3%, which was lower than the 80% cell survival rate reported by Gundry.<sup>34</sup> Studies have shown that *MLH1* can localize to the mitochondria and can inhibit many mitochondrial genes, including *POLG* and *PINK1*, thereby inducing synthetic lethality in MLH1 protein-deficient cells.<sup>35,36</sup> An increase in oxidative DNA lesions (8-oxoG) in the mitochondrial DNA may be responsible for this lethality.<sup>37</sup> Considering that our study used electroporation technology to knock out target genes, similar to Gundry's study,<sup>34</sup> the lower survival rate in this study was mainly related to the function and characteristics of the *MLH1* gene we targeted.

We verified the surviving cell lines after editing at the molecular and protein levels. First, we used Sanger sequencing to screen monoclonal cells. Cell lines with induced mutations in the *MLH1* gene were identified that showed homozygous and heterozygous mutations or bi-allelic mutations with two overlapping traces from the targeting site. Then, we identified two cell lines with complete MLH1 protein deficiency (GM12878Cas9\_6 and GM12878Cas9\_10) using WB. Through NGS sequencing of the two MLH1 protein-deficient cell lines, we verified the mutation pattern of the *MLH1* gene and the changes in the protein amino acid sequences. The results showed that the two MLH1 protein-deficient cell lines had bi-allelic mutations, which produced stop codons to cause termination of protein expression after the introduction of gene mutations. This further explained and verified the results of Sanger sequencing and WB at the genetic level and confirmed the consistency of the genotype and phenotype of the cell lines we established. In clinical practice, among patients with dMMR tumors, 50%-60% of patients exhibit bi-allelic somatic inactivation of the MMR gene (two mutations or one mutation and loss of heterozygosity).<sup>38,39</sup> The mutation patterns of the GM12878Cas9\_6 and GM12878Cas9\_10 cell lines were consistent

with these clinical manifestations, with base changes in two alleles. Our NGS sequencing of the HCT116 immortalized cell line (MLH1 protein-deficient) from patients with colorectal cancer showed that these cells exhibited homozygous bi-allelic mutations, which were the same as the mutations in the GM12878Cas9\_10 cell line. Overall, the mutation characteristics of the MLH1 protein-deficient cell lines we established were similar to those commonly seen in the clinic.

Subsequently, we performed IHC testing on MLH1 protein-deficient cells to verify their feasibility for use in clinical practice. The results showed that the MLH1 protein was completely lost in the GM12878Cas9\_6 and GM12878Cas9\_10 cell lines, showing consistency with the immortalized cell line HCT116 derived from colorectal cancer patients. Based on these observations, we further established a mouse xenograft model to generate FFPE tissue samples and then determined the suitability of these samples for clinical use. In our previous study, we demonstrated that FFPE specimens derived from xenograft tumors are stable and homogeneous and successfully developed *EML4-ALK* FFPE reference materials with histological structures.<sup>31</sup> In this study, based on the same method, we successfully induced tumor formation through xenotransplantation. H&E staining showed that, in contrast to FFPE samples derived from cell lines, FFPE samples of xenograft tumors were highly consistent with clinical specimens from endometrial cancer. Histological analyses demonstrated that FFPE samples from xenograft tumors displayed typical histological structures and histopathological characteristics of tumor tissues, such as tumor infiltration, inflammation, bleeding, and tissue necrosis, providing a complete model of pathological tissue samples. In addition, the tissue IHC results also showed a consistent phenotype with cell lines and clinical samples, in which MLH1 nuclear staining was completely lost. Taken together, these findings proved the feasibility of our established MLH1 protein-deficient FFPE samples from xenograft tumors as a novel QC material for clinical IHC testing. Interestingly, in MLH1 protein-deficient samples, we also observed PMS2 protein deficiency simultaneously, with the loss of nuclear staining. That is, the mutation of *MLH1* caused concurrent loss of MLH1/PMS2, and the cell lines showed the MLH1-/PMS2- phenotype. This phenomenon was consistent with previous studies showing that *MLH1* mutation was accompanied by the loss of PMS2 protein.<sup>7</sup> In the functional state, the MLH1 protein is an obligatory partner of the MLH1/PMS2 heterodimer in the MMR repair process. Abnormality of the MLH1 protein may lead to proteolytic degradation of the dimer, resulting in the loss of PMS2 protein.<sup>15</sup> Therefore, our FFPE QC materials are not only suitable for the detection of MLH1 panels, but also suitable for the detection of PMS2 panels, in which PMS2 is used to determine whether further detection of MLH1 is needed.

In the present study, we have successfully developed a novel QC material for MLH1 protein deficiency testing with ideal properties and that can overcome the limitations of existing QC materials. In contrast to the limitations of patient tumor specimens, our novel FFPE QC material is homogeneous and sustainable and can be stably produced in batches through *in vitro* culture and the establishment of xenograft models. Compared with tumor cell line samples, our QC material

provides a better choice. The edited cell line successfully solves the problem of limited sources of immortalized tumor cell lines derived from patient tumor tissues. An arbitrary series of protein-deficient cell lines can be established by gene editing. Xenotransplantation can also induce typical tissue structures similar to those of clinical samples, which can be used to simultaneously evaluate H&E and IHC staining. Importantly, our novel FFPE QC material can provide quality control for the entire IHC process, including paraffin embedding, slicing, staining, and reporting. This solves the challenges inherent in synthetic protein materials, which can be used to evaluate only a few steps or a single step in IHC tests, such as staining and antigen retrieval. Furthermore, the novel FFPE QC material has broad clinical applicability and can be used in combination with tissue microarray (TMA) and punch biopsy for external and internal quality control. By punch biopsy procedure and pairing with MLH1-positive and MLH-negative cell lines on a single slide, we can add paired on-slide controls to patient tissue slides, which is considered the optimal strategy for routine quality control.<sup>23,40</sup> In addition, the use of paired negative and positive controls also addresses the problem of missing internal controls for some specimens and overcomes the limitation that the stromal cells derived from mice in the QC materials we prepared cannot be stained, such that negative and positive IHC staining could be characterized at the same time to monitor whether the staining was correct.<sup>41</sup> Having a negative control is indispensable in evaluating the analytical specificity of antibodies and laboratory staining procedures.<sup>41</sup> However, samples with completely negative staining for MLH1 protein are difficult to obtain clinically. Our research further addressed this problem by producing a large number of available negative samples and also provides a new approach for establishing negative controls for other protein deficiency testing.

In conclusion, our study successfully established MLH1 protein-deficient cell lines using CRISPR/Cas9 gene editing technology. Through a series of verification methods, it was proven that the MLH1 protein-deficient cell lines we established have *MLH1* gene mutations and protein deficiencies similar to those in clinical samples. By employing xenografting, we developed novel FFPE QC materials with the advantages of homogeneity, sustainable production, and typical histological structures that are suitable for the standardization of the clinical IHC method. Our study provides a new direction for research on QC materials used in clinical laboratory testing.

#### ACKNOWLEDGMENTS

We thank Dr. Wensheng Wei for generously providing the GM12878 cell line stably expressing Cas9 and mCherry for our study. This work was supported by the grants from National Key R&D Program of China 2018YFE0201604 (Jinming Li), the Fund for Beijing Dongcheng District Outstanding Talents Team Program 2019DCT-M-01 (Rui Zhang) and Beijing Hospital Nova Project (BJ-2018-136) (Rui Zhang).

#### CONFLICT OF INTEREST

The authors declare that they have no conflict of interest.

#### DATA AVAILABILITY STATEMENT

Data sharing not applicable to this article as no datasets were generated or analyzed during the current study.

#### ORCID

Jinming Li  <https://orcid.org/0000-0002-1476-3397>

Rui Zhang  <https://orcid.org/0000-0002-3287-4883>

#### REFERENCES

1. Antonia SJ, Villegas A, Daniel D, et al. Durvalumab after chemoradiotherapy in stage III non-small-cell lung cancer. *N Engl J Med*. 2017;377(20):1919-1929.
2. Marcus L, Lemery SJ, Keegan P, et al. FDA approval summary: pembrolizumab for the treatment of microsatellite instability-high solid tumors. *Clin Cancer Res*. 2019;25(13):3753-3758.
3. Chang L, Chang M, Chang HM, et al. Microsatellite instability: a predictive biomarker for cancer immunotherapy. *Appl Immunohistochem Mol Morphol*. 2018;26(2):e15-e21.
4. Le DT, Durham JN, Smith KN, et al. Mismatch repair deficiency predicts response of solid tumors to PD-1 blockade. *Science*. 2017;357(6349):409-413.
5. Ruiz-Bañobre J, Goel A. DNA mismatch repair deficiency and immune checkpoint inhibitors in gastrointestinal cancers. *Gastroenterology*. 2019;156(4):890-903.
6. Pečina-Šlaus N, Kafka A, Salamon I, et al. Mismatch repair pathway, genome stability and cancer. *Front Mol Biosci*. 2020;7:122.
7. Baretta M, Le DT. DNA mismatch repair in cancer. *Pharmacol Ther*. 2018;189:45-62.
8. Cunningham JM, Kim CY, Christensen ER, et al. The frequency of hereditary defective mismatch repair in a prospective series of unselected colorectal carcinomas. *Am J Hum Genet*. 2001;69(4):780-790.
9. Thibodeau SN, French AJ, Cunningham JM, et al. Microsatellite instability in colorectal cancer: different mutator phenotypes and the principal involvement of hMLH1. *Cancer Res*. 1998;58(8):1713-1718.
10. Kato M, Takano M, Miyamoto M, et al. DNA mismatch repair-related protein loss as a prognostic factor in endometrial cancers. *J Gynecol Oncol*. 2015;26(1):40-45.
11. Bischoff J, Ignatov A, Semczuk A, et al. hMLH1 promoter hypermethylation and MSI status in human endometrial carcinomas with and without metastases. *Clin Exp Metastasis*. 2012;29(8):889-900.
12. Truninger K, Menigatti M, Luz J, et al. Immunohistochemical analysis reveals high frequency of PMS2 defects in colorectal cancer. *Gastroenterology*. 2005;128(5):1160-1171.
13. McCarthy AJ, Capo-Chichi JM, Spence T, et al. Heterogenous loss of mismatch repair (MMR) protein expression: a challenge for immunohistochemical interpretation and microsatellite instability (MSI) evaluation. *J Pathol Clin Res*. 2019;5(2):115-129.
14. Sun L, Pfeifer JD. Pitfalls in molecular diagnostics. *Semin Diagn Pathol*. 2019;36(5):342-354.
15. Shia J. Immunohistochemistry versus microsatellite instability testing for screening colorectal cancer patients at risk for hereditary nonpolyposis colorectal cancer syndrome. Part I. The utility of immunohistochemistry. *J Mol Diagn*. 2008;10(4):293-300.
16. Southey MC, Jenkins MA, Mead L, et al. Use of molecular tumor characteristics to prioritize mismatch repair gene testing in early-onset colorectal cancer. *J Clin Oncol*. 2005;23(27):6524-6532.
17. Bartley AN, Luthra R, Saraiya DS, et al. Identification of cancer patients with Lynch syndrome: clinically significant discordances and problems in tissue-based mismatch repair testing. *Cancer Prev Res (Phila)*. 2012;5(2):320-327.

18. Müller W, Burgart LJ, Krause-Paulus R, et al. The reliability of immunohistochemistry as a prescreening method for the diagnosis of hereditary nonpolyposis colorectal cancer (HNPCC)—results of an international collaborative study. *Fam Cancer*. 2001;1(2):87-92.
19. Kim SW, Roh J, Park CS. Immunohistochemistry for pathologists: protocols, pitfalls, and tips. *J Pathol Transl Med*. 2016;50(6):411-418.
20. Janardhan KS, Jensen H, Clayton NP, et al. Immunohistochemistry in investigative and toxicologic pathology. *Toxicol Pathol*. 2018;46(5):488-510.
21. Consensus on the detection of microsatellite instability in colorectal cancer and other related solid tumors in China. *Zhonghua Zhong Liu Za Zhi*. 2019;41(10):734-741.
22. Torlakovic EE. Quality control by tissue microarray in immunohistochemistry. *J Clin Pathol*. 2012;65(10):961.
23. Cates JM, Troutman KA Jr. Quality management of the immunohistochemistry laboratory: a practical guide. *Appl Immunohistochem Mol Morphol*. 2015;23(7):471-480.
24. Xiao Y, Gao X, Maragh S, et al. Cell lines as candidate reference materials for quality control of ERBB2 amplification and expression assays in breast cancer. *Clin Chem*. 2009;55(7):1307-1315.
25. Li Y, Zhang R, Han Y, et al. Comparison of the types of candidate reference samples for quality control of human epidermal growth factor receptor 2 status detection. *Diagn Pathol*. 2016;11(1):85.
26. Sompuram SR, Kodala V, Zhang K, et al. A novel quality control slide for quantitative immunohistochemistry testing. *J Histochem Cytochem*. 2002;50(11):1425-1434.
27. Hötzel KJ, Havnar CA, Ngu HV, et al. Synthetic antigen gels as practical controls for standardized and quantitative immunohistochemistry. *J Histochem Cytochem*. 2019;67(5):309-334.
28. Lin G, Zhang K, Peng R, et al. Clustered regularly interspaced short palindromic repeat (CRISPR)/CRISPR-associated endonuclease Cas9-mediated homology-independent integration for generating quality control materials for clinical molecular genetic testing. *J Mol Diagn*. 2018;20(3):373-380.
29. Jia S, Zhang R, Lin G, et al. A novel cell line generated using the CRISPR/Cas9 technology as universal quality control material for KRAS G12V mutation testing. *J Clin Lab Anal*. 2018;32(5):e22391.
30. Zhou L, Li R, Zhang R, et al. Utilizing CRISPR/Cas9 technology to prepare lymphoblastoid cell lines harboring genetic mutations for generating quality control materials in genetic testing. *J Clin Lab Anal*. 2020;34(7):e23256.
31. Peng R, Zhang R, Lin G, et al. CRISPR/Cas9 technology-based xenograft tumors as candidate reference materials for multiple EML4-ALK rearrangements testing. *J Mol Diagn*. 2017;19(5):766-775.
32. Drost J, van Boxtel R, Blokzijl F, et al. Use of CRISPR-modified human stem cell organoids to study the origin of mutational signatures in cancer. *Science*. 2017;358(6360):234-238.
33. Nelson GS, Pink A, Lee S, et al. MMR deficiency is common in high-grade endometrioid carcinomas and is associated with an unfavorable outcome. *Gynecol Oncol*. 2013;131(2):309-314.
34. Gundry MC, Brunetti L, Lin A, et al. Highly efficient genome editing of murine and human hematopoietic progenitor cells by CRISPR/Cas9. *Cell Rep*. 2016;17(5):1453-1461.
35. Martin SA, Hewish M, Sims D, et al. Parallel high-throughput RNA interference screens identify PINK1 as a potential therapeutic target for the treatment of DNA mismatch repair-deficient cancers. *Cancer Res*. 2011;71(5):1836-1848.
36. Mishra M, Kowluru RA. Retinal mitochondrial DNA mismatch repair in the development of diabetic retinopathy, and its continued progression after termination of hyperglycemia. *Invest Ophthalmol Vis Sci*. 2014;55(10):6960-6967.
37. Rashid S, Freitas MO, Cucchi D, et al. MLH1 deficiency leads to deregulated mitochondrial metabolism. *Cell Death Dis*. 2019;10(11):795.
38. Rigger LS, Snaebjornsson P, Rosenberg EH, et al. Double somatic mutations in mismatch repair genes are frequent in colorectal cancer after Hodgkin's lymphoma treatment. *Gut*. 2018;67(3):447-455.
39. Pearlman R, Frankel WL, Swanson B, et al. Prevalence and spectrum of germline cancer susceptibility gene mutations among patients with early-onset colorectal cancer. *JAMA Oncol*. 2017;3(4):464-471.
40. Bragoni A, Gambella A, Pigozzi S, et al. Quality control in diagnostic immunohistochemistry: integrated on-slide positive controls. *Histochem Cell Biol*. 2017;148(5):569-573.
41. Hewitt SM, Baskin DG, Frevert CW, et al. Controls for immunohistochemistry: the Histochemical Society's standards of practice for validation of immunohistochemical assays. *J Histochem Cytochem*. 2014;62(10):693-697.

**How to cite this article:** Li R, Zhang R, Tan P, et al. Development of novel quality control material based on CRISPR/Cas9 editing and xenografts for MLH1 protein deficiency testing. *J Clin Lab Anal*. 2021;35:e23746. <https://doi.org/10.1002/jcla.23746>